Spectroscopic assignments of Ti^{3+} and Ti^{4+} in titanium-doped OH^- free low-silica calcium aluminosilicate glass and role of structural defects on the observed long lifetime and high fluorescence of Ti^{3+} ions

L. H. C. Andrade*
Grupo de Espectroscopia Óptica e Fototérmica, Universidade Estadual de Mato Grosso do Sul–UEMS, C.P. 351, CEP 79804-970, Dourados, MS, Brazil and Laboratoire de Physico-Chimie des Matériaux Luminescents, Université de Lyon, Université Claude Bernard Lyon 1, UMR 5620 CNRS, 69622, Villeurbanne, France

S. M. Lima
Grupo de Espectroscopia Óptica e Fototérmica, Universidade Estadual de Mato Grosso do Sul–UEMS, C.P. 351, CEP 79804-970, Dourados, MS, Brazil

A. Novatski
Departamento de Física, Universidade Estadual de Maringá, Av. Colombo 5790, 87020-900, Maringá, PR, Brazil and Laboratoire de Physico-Chimie des Matériaux Luminescents, Université de Lyon, Université Claude Bernard Lyon 1, UMR 5620 CNRS, 69622 Villeurbanne, France

A. M. Neto, A. C. Bento, and M. L. Baesso
Departamento de Física, Universidade Estadual de Maringá, Av. Colombo 5790, 87020-900 Maringá, PR, Brazil

F. C. G. Gandra
Departamento de Eletrônica Quântica, Instituto de Física Gleb Wataghin, Universidade Estadual de Campinas, Cidade Universitaria, 13083-970, Campinas, SP, Brazil

Y. Guyot and G. Boulon
Laboratoire de Physico-Chimie des Matériaux Luminescents, Université de Lyon, Université Claude Bernard Lyon 1, UMR 5620 CNRS, 69622 Villeurbanne, France

(Received 14 January 2008; revised manuscript received 13 May 2008; published 15 December 2008)

In this work we present the spectroscopic assignments of Ti^{3+} and Ti^{4+} in titanium-doped OH^- free low-silica calcium aluminosilicate glass and the influence of structural defects on the observed long lifetime and high fluorescence intensity of Ti^{3+} ions. Measurements were performed with electron-spin resonance (ESR), time resolved luminescence, ultraviolet-visible (UV-VIS) optical excitation and emission spectra, and conventional optical absorption and photoconductivity. The ESR data showed that the Ti^{3+}/Ti^{4+} ratio increases with the doping concentration and that the Ti^{3+} ions are in distorted octahedral sites. The assignment of the Ti^{3+} and Ti^{4+} emission bands derived from the spectroscopic results allowed us to propose a model explaining the mechanisms involved in the luminescence processes. The long lifetime of the Ti^{3+} emission around 650 nm (on the order of 170 μs) is about two orders of magnitude higher than the values found in the literature and was associated to the trapping of the excited electrons by the glass defects followed by detrapping via defect recombination. In conclusion, the combination of several techniques permitted a comprehensive characterization of the Ti ions in this OH^- free glass.

DOI: 10.1103/PhysRevB.78.224202 PACS number(s): 78.55.Qr, 61.43.Fs, 74.25.Gz, 76.30.Da

I. INTRODUCTION

In a recent paper[1] we reported the development of Ti^{3+}-doped OH^- free low-silica calcium aluminosilicate (LSCAS) glass with broad emission band from about 500 to 800 nm and fluorescence lifetime about two orders of magnitude higher than those of known Ti^{3+}-doped crystals or glasses. This observation deserves special attention due to the fact that the synthesis of trivalent titanium in glass is a difficult task to be accomplished. In addition, previous results showed that transition metals in the $3d^1$ electronic configuration usually do not exhibit long fluorescence lifetime due to the allowed electronic transition and the high sensitivity to the crystal field. The low lifetime value for this kind of system is known to be a drawback in terms of obtaining inversion in the population of the involved electronic level. On the other hand, an important remark that has motivated the study of the $3d^1$ electronic configuration energy levels is the absence of excited-state absorption as observed in several materials doped with Ti^{3+}, V^{4+}, Cr^{5+}, and Mn^{6+} (Refs. 2–5) that has been associated with high optical gain from visible (VIS) to near infrared (NIR),[6,7] broad emission band,[8,9] ultrashort time switch,[10] and high fluorescence quantum efficiency.[11–14]

The presence of other valence states of transition metals than the desirable $3d^1$ electronic configuration is probably the main challenge for the synthesis of solid-state materials doped with transition metals prepared at high temperatures. Concerning Ti doping in oxide materials, the presence of Ti^{3+}, Ti^{4+}, and Ti^{3+}-Ti^{4+} pairs defines the optical properties

of the obtained samples. For example, the generation of excited-state absorption of the electronic excited-state ^2E levels of Ti^{4+} or the direct parasitic broadband near infrared absorption around 800 nm are associated to pairs of Ti^{3+}-Ti^{4+}.[15–19] The main characteristic of Ti^{4+} ion is the broad blue emission band as observed in $Ti:MgAl_2O_4$ (Ref. 20) and $Ti:YAlO_3$,[21] which originated from charge transfer between Ti^{4+} and oxygen bridging. This emission band has been the subject of interest in the search for tunable solid-state lasers in the blue spectral region.[20]

Therefore, the interpretation of the mechanisms involved in the observed emission of our Ti-doped samples demands the knowledge of the glass structure such as ion coordination and the matrix defect distribution. Then, the purpose of this work is to investigate the mechanisms involved in the photoluminescence processes in the TiO_2-doped LSCAS. To do that, two sets of samples with different TiO_2 concentration were prepared and analyzed by the following techniques: optical absorption (OA), UV-VIS optical excitation (OEx) and emission spectra (OEm), time resolved luminescence (TRL), electron-spin resonance (ESR) and photoconductivity. In addition, the basicity of the samples was calculated by the Duffy model,[22] which was used to explain the related equilibrium between Ti^{3+} and Ti^{4+} ions in the glass.

II. EXPERIMENT

A. Glass preparation and characteristics

The samples were prepared with high grade of purity oxides in wt %. The first set of glasses was melted with 41.5% of Al_2O_3 (5N), 47.4% of CaO (5N), 7% of SiO_2 (5N), and $4.1-X$% of MgO (5N) with $X=0$, 0.25, 0.5, 1.0, 1.5, 2.0, 2.5, 3.0, and 3.5% of TiO_2 (4N). The second set composition was $41.5-Y$% of Al_2O_3 (5N), 47.4% of CaO (5N), 7% of SiO_2 (5N), and 4.1% of MgO (5N) with $Y=0$, 0.25, 0.5, 1.0, 1.5, 2.0, 2.5, 3.0, and 3.5% of TiO_2 (4N). The mixtures were melted under vacuum atmosphere at 1600 °C for 2 h. This procedure was adopted to remove the presence of OH^- from the sample and was our route to obtain a high ratio of Ti^{3+} oxidation state in the glass. The samples were polished with optical finishing according to the used technique.

Previous thermomechanical and optical characterizations of this OH^- free low-silica calcium aluminosilicate glass have shown its excellent properties such as phonon energy on the order of 780 cm^{-1}, which is lower than those of phosphate, silicate, and germanate glasses;[23] high thermal-conductivity values of about 1.5 $W(m\ K)^{-1}$; and glass transition temperature (T_g) at approximately 850 °C.[24] This glass also presents high IR transmission (up to 6 μm) (Ref. 25) and high resistance to laser damage.[26] In addition, LSCAS glass doped with several rare-earth cations[27–29] was shown to be a promising host for laser applications.

B. Methods of characterization

The OA experiments were recorded at room temperature using a UV-VIS-NIR Perkin Elmer Lambda 900 spectrophotometer using samples with average thicknesses of about 0.5 mm. The OEx experiments were carried out using a 450W Xe^+ lamp and a H10D Jobin Yvon monochromator. OEm was collected by an optical fiber and analyzed by a Triax 320 Jobin Yvon monochromator with a 600 grooves/mm grating (resolution of 0.05 nm) and a Peltier cooled charge coupled device (CCD) detector. The first step was the determination of the emission spectra dependence on the scanning excitation wavelengths from 200 to 450 nm. We used 5 nm steps and recorded the optical emission for each excitation. This experimental procedure allowed us to identify the spectral region with the most intense emission generated from different excitations. Knowing the emission region we fixed the wavelength in the monochromator and recorded the emission from the sample by scanning the excitation wavelength with the Xe^+ lamp coupled in a second monochromator. The obtained excitation spectra were normalized by the lamp emission spectra. This method permits one to perform deconvolution of the optical-absorption spectra and to assign the observed emission to each excitation band.

TRL experiments were carried out to obtain the temporal behavior of the emission decay. The samples were excited with third or fourth harmonics of a pulsed $Nd^{3+}:YAG$ laser Spectra Physics Quanta-Ray GCR130, which delivers pulses of 10 Hz with 10 ns of time length and 0.1 cm^{-1} spectral width. The emission of the sample was analyzed by an Oriel f-125 monochromator with a grating of 400 grooves/mm and detected by an Instaspec V detector combined with a gate intensified CCD camera calibrated with an Hg fluorescent lamp. The temperature dependence lifetime was performed with the sample fixed at a cold finger of a nitrogen cryostat coupled with a temperature system control from 77 to 400 K and the lifetime acquisition was made as described in Ref. 1. The samples were cooled down at 10 K and slowly heated until 400 K. The lifetime values were calculated by using the integration method as described in Ref. 30.

The ESR instrument used was a homemade set up operating at 9.5 GHz in the X band, and the measurements were performed at both room and low temperatures (at 8 K). The photoconductivity measurements were carried out as described in Ref. 31.

III. RESULTS AND DISCUSSION

A. Spectroscopic characterization of color centers in the undoped and TiO_2 doped glasses

Figure 1 shows the optical-absorption spectra measured in the LSCAS samples that were obtained by exchanging MgO by TiO_2. The spectral range was from 200 to 1000 nm. The intense and very broad absorption in the UV region is a result of superimposed bands from Ti^{3+} and Ti^{4+} ions.[16,33] There is also a broad absorption band near 540 nm that has a tail extending to the near infrared region, which may be related to Ti^{3+}-Ti^{4+} ion pair interactions.[16,32,34] As a characteristic of these absorption bands, a deep brown coloration was observed in the prepared samples at concentrations above 1% TiO_2. The deconvolution of the absorption spectra and the assignment of the mentioned optical-absorption bands to each Ti ion will be presented later on in this paper. The results for the second set of samples showed the same characteristics; hence, it will not be shown.

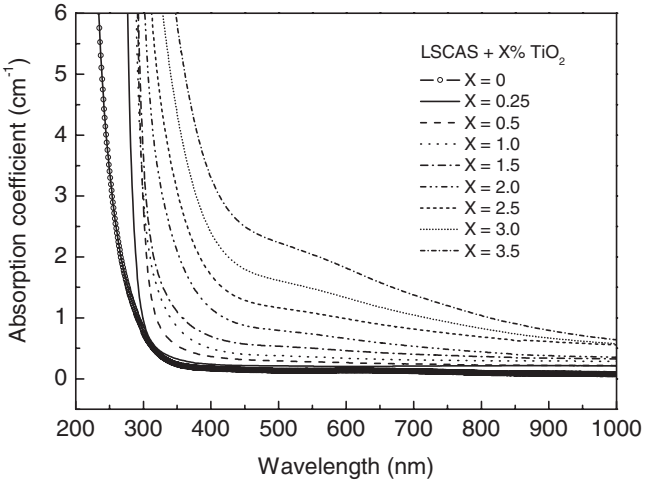

FIG. 1. Optical-absorption spectra for the LSCAS glass as a function of TiO_2 concentration.

In order to obtain a full picture of the excitation and emission spectra in the undoped LSCAS sample we performed several luminescence experiments with different excitation wavelengths. From that we constructed an image plot of the emission against the excitation wavelengths as shown in Fig. 2(a). The emission intensities are represented by the color pattern shown in the right-side scale. The observed fluorescence centered at 430 nm for excitation at 249 nm is due to lattice defects such as F color centers.[18] The barycenter of the emission bands was constant with the variation in the excitation wavelength, indicating the existence of only one kind of color center occupying different sites. Figure 2(b) shows the emission and excitation spectra of the marked position in the contour plot, illustrating the band form. The excitation spectrum was obtained by recording the emission at 440 nm and the emission spectrum excited at 240 nm. The fitting of the excitation spectrum with a single Gaussian function (solid line) evidenced its symmetrical shape reinforcing the existence of only F kind color centers. Similar fitting procedures were also performed taking into account excitation spectra recorded at 420 and 450 nm, giving always a single Gaussian behavior. Another evidence of F color center in the natural disorder of these sites in the glass was verified by observing the nonexponential decay of the emission at 430 nm (shown in Fig. 3), which was calculated by the integral method[30] resulting in a value of 18 μs.

Next, the undoped sample was irradiated with the third harmonic of the Nd^{3+}:YAG laser at 355 nm for 10 min. The induced change in the optical-absorption spectrum is shown in Fig. 4. The presence of a new absorption band in the UV-blue regions illustrates the photochromism of this glass similarly to what has been shown previously.[35,36] Repeating the emission and excitation experiments in this irradiated sample using the same procedure described before, two emission centers are now observed. The first at 425 nm corresponds to the 249 nm excitation [Fig. 5(a)] similar to that of Fig. 2, while that at 535 nm, corresponding to the 323 nm excitation [Fig. 5(b)], is a new emission band which is very weakly (at the maximum peak position) generated after the sample irradiation. The excitation spectrum is very noisy and

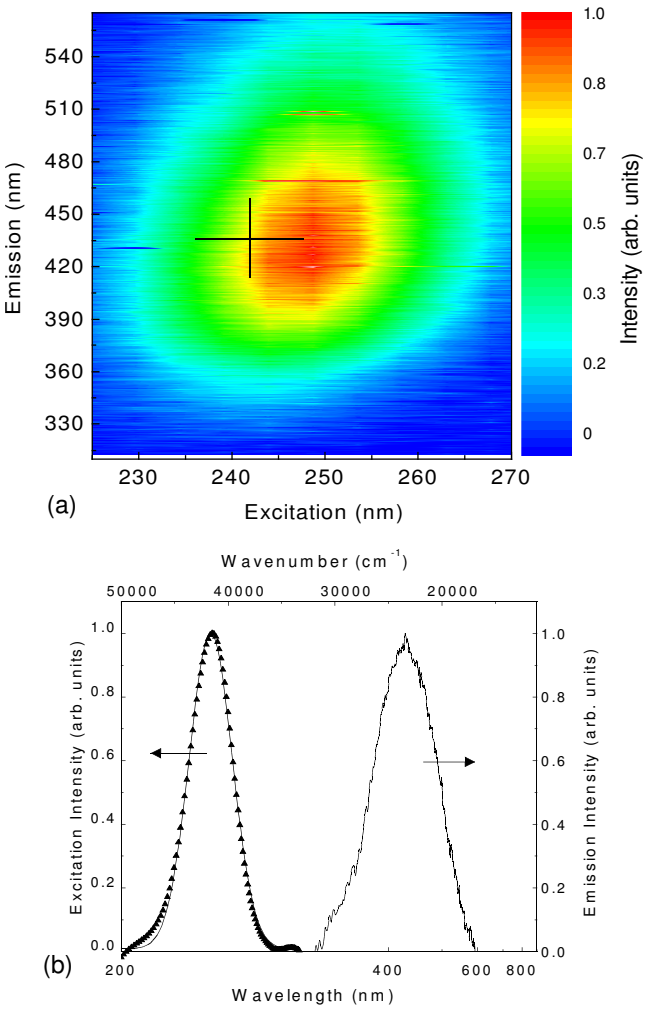

FIG. 2. (Color online) Image plot of the emission vs excitation spectra (a) for several wavelengths, and excitation vs emission spectra (b) for the undoped LSCAS. The marked position in the image plot (a) indicates the respective region of excitation and emission of the spectra shown in (b).

as a consequence it was not possible to estimate the fast lifetime value with precision. This observation confirms the generation of additional color centers in the lattice, which

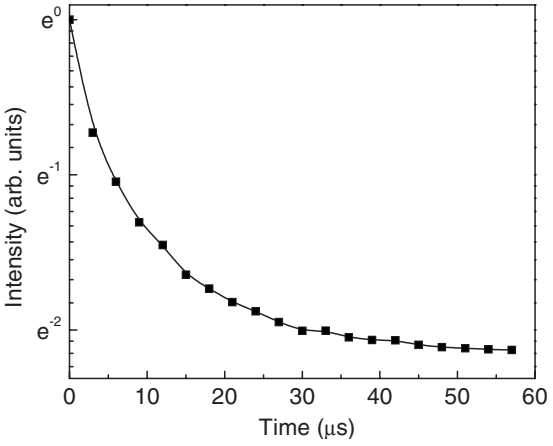

FIG. 3. Undoped LSCAS luminescence decay at 431 nm under 266 nm excitation.

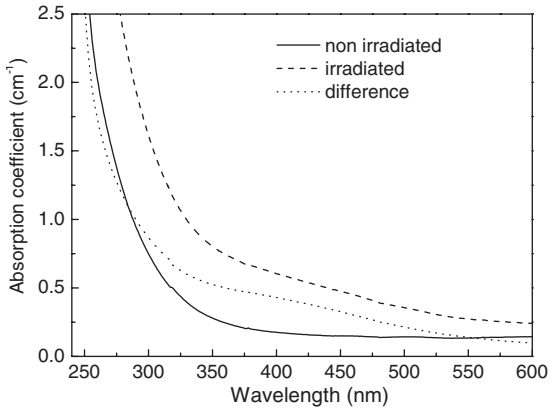

FIG. 4. Optical-absorption spectrum of the undoped LSCAS: before irradiation (black line) and after 10 min of irradiation with 355 nm (dashed line). The dotted line is the difference between the two spectra.

can be attributed to F^+ color centers created by ionization during the sample radiation. In this case, the electrons from O^{2-} can be removed by the laser radiation and trapped in the neighbor vacancies. Similar results were obtained and associated to the color centers in pure $MgAl_2O_4$ spinel crystals[20] whose emission centers were observed at 450 and 720 nm for excitations around 350 and 270 nm, respectively.

Figure 6 shows the image plot and the emission and excitation spectra for the 1.5 wt % TiO_2-doped LSCAS sample. It is possible to observe two emission bands: one centered at 490 nm for excitation wavelength at 270 nm [Fig. 6(a)] and the other at 650 nm for excitation at 330 nm [Fig. 6(b)]. These emission peaks are much more intense than that observed in the undoped sample. Furthermore, there is a small shift in the center position of both emission and excitation spectra in comparison with those from the color centers in the undoped glass showed in Fig. 5. Since the excitation spectrum close to 270 nm exhibits a nonsingle Gaussian behavior, the fitting was performed in energy scale. To do that we used a Gaussian curve with the parameters from the F color centers obtained in Fig. 2, with the maximum at 240 nm, and a second Gaussian centered at 271 nm, which is attributed to Ti^{4+} ion emission as will be demonstrated in Secs. III B and III F. This strong UV absorption band has been associated to charge-transfer processes between Ti^{4+} and O^{2-} ions by the two possible molecular transitions $t_{1u}(\pi^b) \rightarrow t_{2g}(\pi^*)$ or $t_{2u}(\pi) \rightarrow t_{2g}(\pi^*)$ as observed by Yamaga *et al.*[18,37] in Ti-doped Al_2O_3 crystals. Considering the intrinsic excitation band in the nonirradiated LSCAS-undoped sample, we detected only one broad emission band with the maximum at 486 nm. Then, we believe that this emission is related to just one of these expected transitions for Ti^{4+} ions as can be seen in Fig. 6(a). The broad emission band at 650 nm obtained under pumping at 330 nm [Fig. 6(b)] is assigned to Ti^{3+} ions. The presence of these ions in the samples will be confirmed later by the ESR measurements. This red emission is less pronounced than that in the blue region. The fitting of the excitation spectra was performed with a single Gaussian function. This band has been attributed to the transition $^2E \rightarrow {}^2T_2$ from the Ti^{3+} ions in an octahedral site.[38]

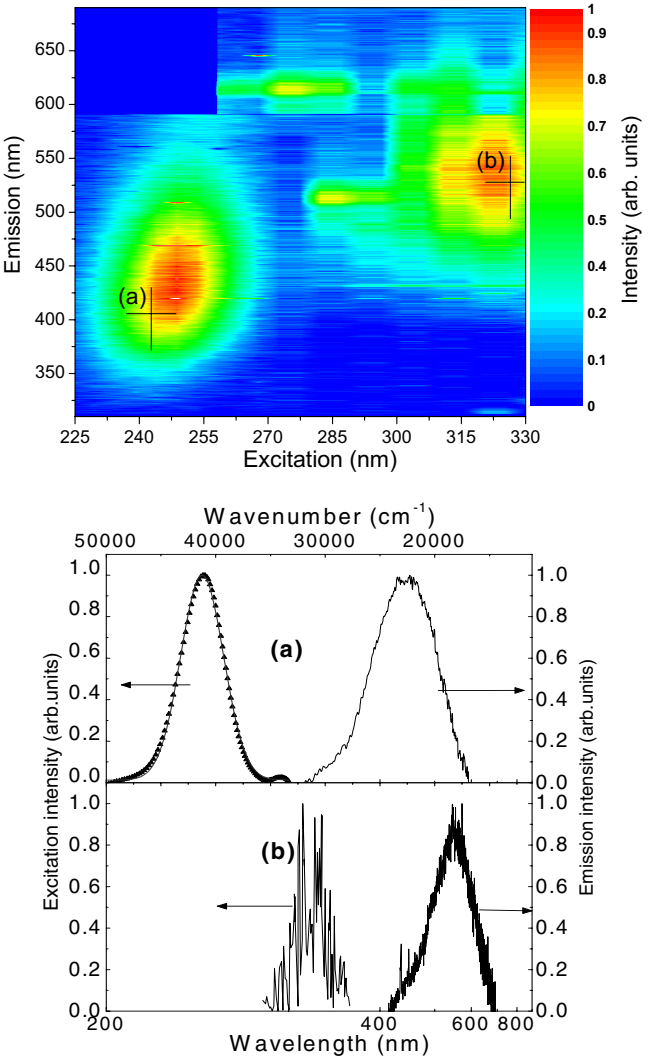

FIG. 5. (Color online) Image plot of the emission vs excitation spectra for several wavelengths of the irradiated undoped LSCAS samples. The plot shows (a) the luminescence and the excitation spectra at 431 and 241 nm, respectively, and (b) the luminescence and excitation spectra at 527 and 325 nm, respectively. The Gaussian fit in (a) was performed for the respective marked regions in the image plots (a) and (b), respectively.

Basun *et al.*[17] reported similar results for the emission and excitation spectra of Ti^{3+} and Ti^{4+} ions in Ti-doped YAP perovskite.

Figure 7 shows the contour plot and the excitation and emission spectra for the sample with 3.5 wt % of TiO_2. The peaks around $\lambda_{ex}=340$ nm and $\lambda_{em}=650$ nm in Fig. 7(a) are related to Ti^{3+} ions, while those around $\lambda_{ex}=270$ nm and $\lambda_{em}=480$ nm in Fig. 7(b) are attributed to Ti^{4+} ions, similar to those observed for the 1.5 wt % TiO_2 glass. This intense orange emission, as already shown in Ref. 1, confirms the formation of high concentration of Ti^{3+} ions in the glass, showing that the ratio Ti^{3+}/Ti^{4+} increased as a function of the doping concentration. An interesting feature of this orange emission, full width at half maximum (FWHM) of 4237 cm^{-1}, is that it is broader than those of other materials doped with $3d^1$ transition metals such as the traditional

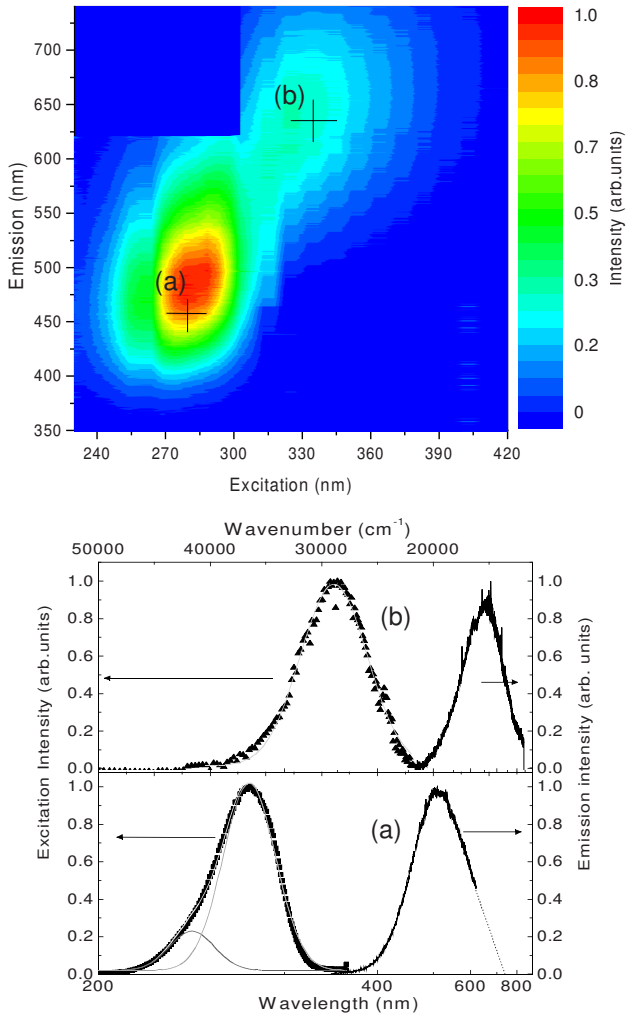

FIG. 6. (Color online) Image plot of the emission as a function of the excitation of LSCAS doped with 1.5 wt % of TiO_2. In (a) the UV excitation and blue emission for Ti^{4+} charge transfer are shown. Below the excitation band the two components fitting with two Gaussians are shown—one attributed to the undoped sample color center and the other related to Ti^{4+} charge transfer. In (b) the excitation and emission bands for the orange emission attributed to Ti^{3+} ions are shown.

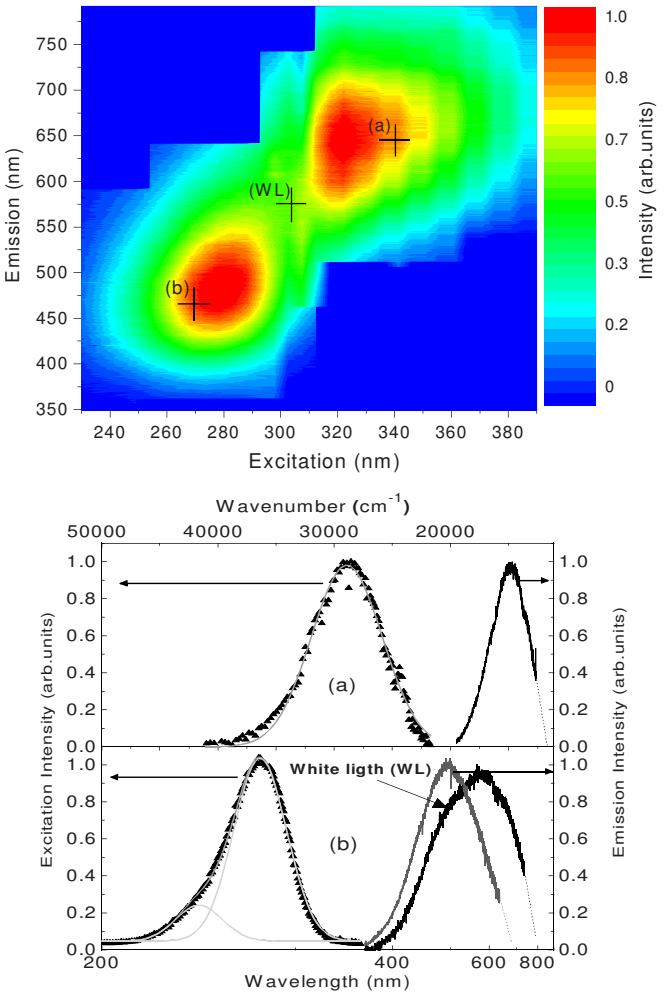

FIG. 7. (Color online) Image plot of the emission as a function of the excitation of the LSCAS with 3.5 wt % of TiO_2. In (a) the excitation and emission bands for orange emission are attributed to Ti^{3+} ions. In (b) the UV excitation and blue emission associated to Ti^{4+} charge transfer are shown. Below the excitation band the two components fitting with two Gaussians are shown—one is attributed to the undoped sample color center, while the other is related to the Ti^{4+} charge-transfer band. The generation of white light for 300 nm excitation is also shown.

$Ti^{3+}:Al_2O_3$ crystal[39] (FWHM of 3200 cm^{-1}), and $Cr^{5+}:SiO_2$ glass (FWHM of 4200 cm^{-1}).[40] The peak position of this band is also comparable to that of some crystals such as $Ti^{3+}:YAlO_3$.[41] Our system presents the emission band shifted toward shorter wavelengths in comparison with the $Ti^{3+}:Al_2O_4$ crystal as shown in Fig. 8. This result is similar to those shown in Ref. 1 for LSCAS doped with 2.0 wt % TiO_2. Another interesting fact observed from the contour plot of Fig. 7 is the generation of white light (WL) in the sample under excitation by 300 nm. Figure 9(a) shows the TRL data under excitation at 266 nm performed with the fourth harmonic of the $Nd^{3+}:YAG$ laser. In this case only the energy levels involving charge transfer of Ti^{4+} and O^{2-} are excited, which results in a luminescence band centered around 470 nm. The fact that the curve shape is similar for different time delay intervals reveals again that the emission originated from a single excited level. Figure 9(b) represents the luminescence decay showing a nonsingle exponential behavior. The decay was fitted with two exponential components with values of 0.7 and 5.6 μs. According to Wong *et al.*[15] these slow and fast components are associated to the nonlocal and local charges compensated of Ti^{4+}, respectively. This charge compensation is related with the average distance between the Ti^{4+} and the glass cations. Under excitation at 355 nm with the third harmonic of the $Nd^{3+}:YAG$ laser, the TRL data for this sample show the same shape for different time delay intervals similar to that observed for the 2.0 wt % TiO_2 LSCAS glass described in Ref. 1. This is a characteristic result of a single excited level. Figure 10 shows the average lifetime values of the 2 wt % TiO_2-doped LSCAS as a function of temperature, which were calculated by the integral method. A considerable increase from about 90 to 1800 μs was observed when the sample temperature was varied from 400 to 77 K. In our previous paper[1] this long

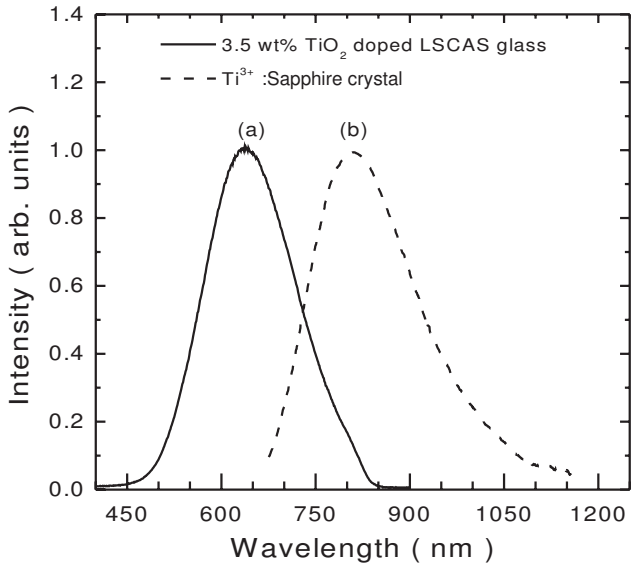

FIG. 8. Luminescence spectra at room temperature of (a) 3.5 wt % of TiO_2 LSCAS glass under excitation at 355 nm; (b) Ti-sapphire crystal (Ref. 39).

lifetime was associated with the interaction of Ti^{3+} ions with structural defects, similar to materials that present mechanoluminescence effects such as Ti^{4+},[42] Eu^{2+},[43] and Ce^{3+} (Ref. 44) doped systems. Further evaluation of this long decay-

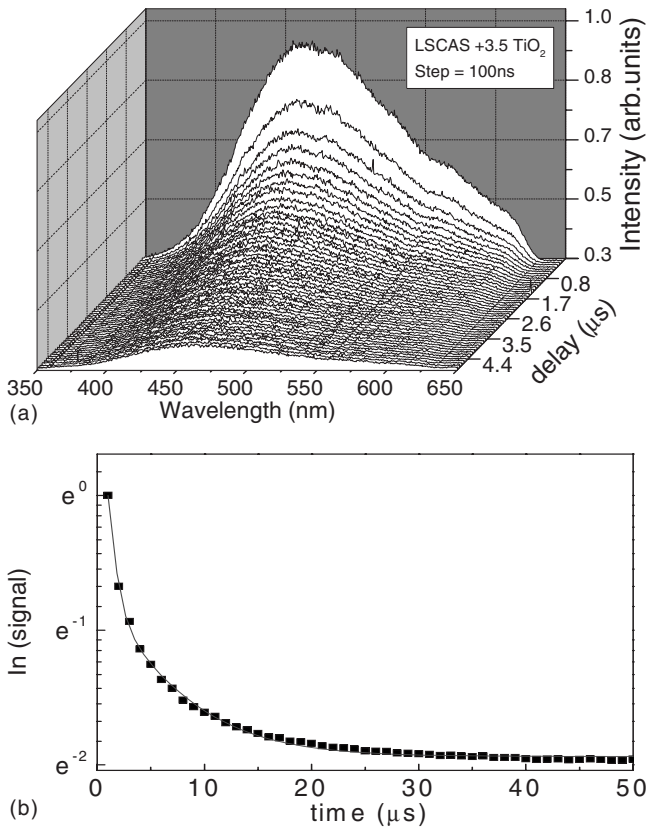

FIG. 9. (a) Time resolved luminescence spectra of the 3.5 wt % TiO_2 LSCAS under 266 nm excitation with initial delay time of 100 ns and steps between acquisitions of 100 ns. (b) Blue luminescence time dependence measured at 486 nm.

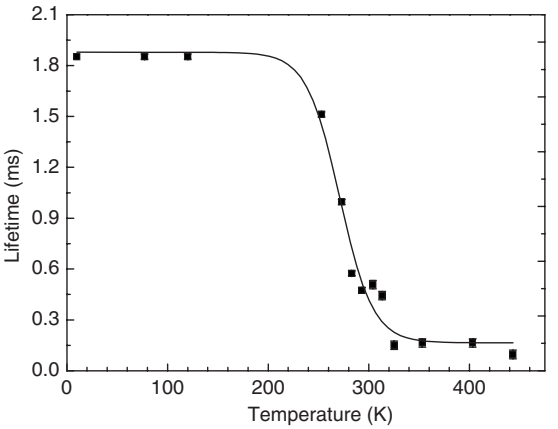

FIG. 10. Lifetime values as a function of temperature for emission at 630 nm of the 3.5 wt % TiO_2 LSCAS.

time behavior will be given later on in this paper.

B. Evidence of Ti^{3+} ions in LSCAS glass by ESR analysis

We performed electron-spin resonance in order to get confirmation of the presence of Ti^{3+} ions in the samples. Figure 11 shows the ESR spectra for the undoped, 1.5, and 2.0 wt % TiO_2 concentration samples measured at room temperature and at 8 K for the 2.0 wt % sample. The resonance line with $g=1.96$ is related to the Ti^{3+} ions in octahedral sites.[45–47] The data for the low-temperature region (at 8 K) show an increase in the resonance line amplitude with no evidence of additional Ti^{3+} sites. The asymmetric curves for all data are due to coordination distortion of the octahedral Ti^{3+} sites as previously reported.[46,47] Figure 12 shows the integrated area of the ESR absorption spectra as a function of the TiO_2 doping concentration, demonstrating that the Ti^{3+}/Ti^{4+} ratio becomes higher when the doping concentration is increased. Previous results have shown that glasses with higher acid compositions favor the reduction in Ti^{4+} to Ti^{3+}.[48] Thus the change in the glass basicity with the increas-

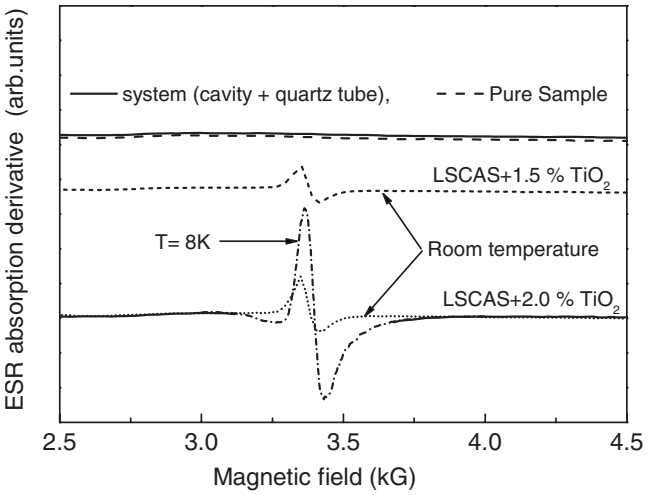

FIG. 11. ESR spectra of the system (without sample)—undoped LSCAS. ESR of doped LSCAS at room-temperature with 1.5 and 2.0 wt % of TiO_2 and at 8 K for the 2.0 wt % doped.

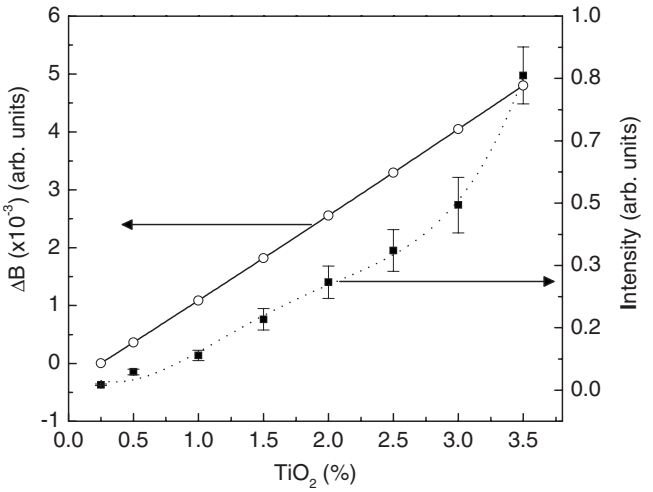

FIG. 12. ESR absorption spectra areas and the optical basicity variation as a function of TiO_2 doping concentration.

ing concentration of TiO_2 may help our analysis.

C. Basicity analysis as a tool to estimate Ti^{3+}/Ti^{4+} ratio

The concept of optical basicity related with the ability of oxygen to donate negative charge was proposed by Duffy *et al.*[22] This "electron donor power" is dependent on the kind of bonding between O^{2-} and the surrounding cations. The more intense the covalent bonding is, the less able is the oxygen to donate charge to an ion in the glass—meaning a lower optical basicity. The glass optical basicity can be written as[22]

$$\Lambda_{(\text{glass})} = X_1\Lambda_1 + X_2\Lambda_2 + \ldots, \tag{1}$$

in which X_1, X_2 are the equivalent fraction of the oxides with each one of them having an optical basicity of Λ_1, Λ_2. The values of Λ_1, Λ_2 used in this work were obtained from Ref. 22.

Table I shows the basicity calculated for each concentration of TiO_2. It can be observed that by increasing the TiO_2 concentration, the glass basicity decreases, favoring the increase in $[Ti^{3+}]$ concentration in relation to $[Ti^{4+}]$. In terms of reaction, the concentration of Ti^{3+} is proportional to TiO_2 doping content; thus,

$$[Ti^{3+}] = C[TiO_2], \tag{2}$$

$$C \propto \Delta B, \tag{3}$$

and

$$\Delta B = B_0 - B. \tag{4}$$

Here, B_0 and B are the optical basicity of the undoped and doped samples, respectively. The values of ΔB for each sample are shown in Table I. Figure 12 shows these data and the integrated area of ESR spectra for each TiO_2 concentration. It can be seen that ΔB increases linearly with the replacement of [MgO] by $[TiO_2]$. These results are consistent

TABLE I. Basicity parameters as a function of TiO_2 and MgO concentration.

Oxides			
MgO (wt %)	TiO_2 (wt %)	Basicity	ΔB (1×10^{-3})
4.1	0	0.8329	0
3.85	0.25	0.8325	0.003
3.6	0.5	0.8321	0.300
3.1	1.0	0.8314	1.088
2.6	1.5	0.8311	1.818
2.1	2.0	0.8299	2.555
1.6	2.5	0.8292	3.298
1.1	3.0	0.8285	4.047
0.6	3.5	0.8277	4.803

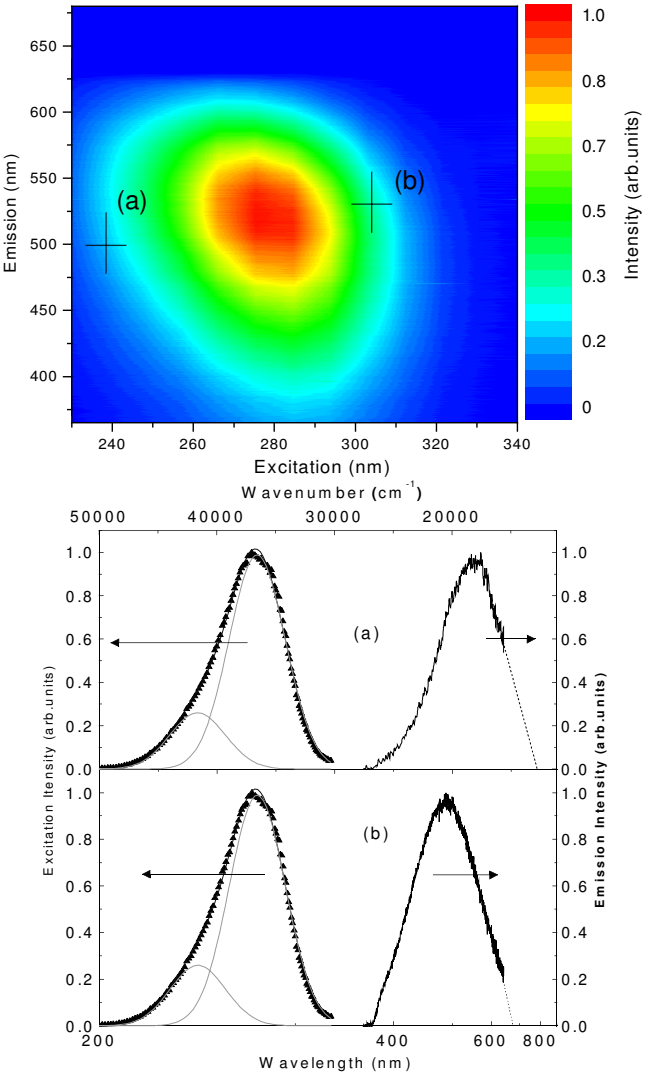

FIG. 13. (Color online) Image plot of both excitation and emission spectra of the 2.0 wt % TiO_2 LSCAS after annealing performed in air atmosphere and at 850 °C for 24 h. In (a) the excitation band of 300 nm and the blue emission centered at 460 nm are shown. In (b) the emission band under excitation at 320 nm is shown.

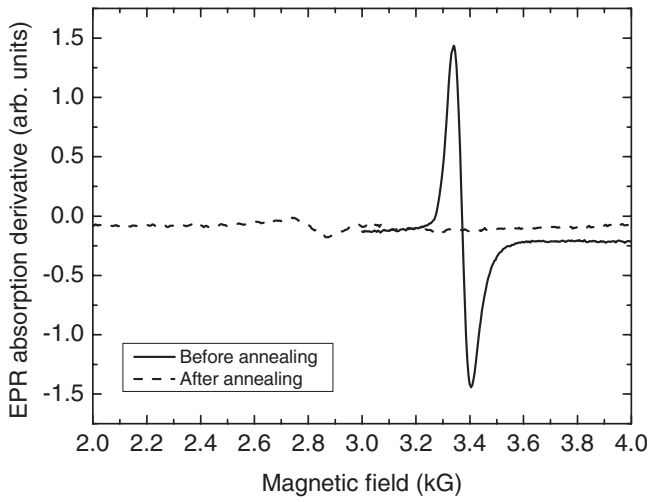

FIG. 14. ESR results at room temperature of the 2.0 wt % of TiO_2 LSCAS before and after annealing.

with the behavior of the integrated areas of the ESR spectra with the TiO_2 amount used in the formulation, showing a nonlinear increase in Ti^{3+} ions in the glass as a function of the doping concentration.

D. Converting Ti^{3+} into Ti^{4+} by annealing procedure

In order to confirm the attribution of the λ_{em}=480 nm blue emission band with its respective λ_{ex}=270 nm UV excitation to Ti^{4+} charge energy transfer and the 650 nm red emission with its respective 340 nm excitation to Ti^{3+} ions, we performed an annealing in air atmosphere, at 850 °C, for 24 h in the 2.0 wt % TiO_2 LSCAS glass. The brownish color due to Ti^{3+} was significantly reduced by the heat treatment. The new emission and excitation spectra for the annealed sample are shown in Fig. 13. It can be observed that the emission and excitation spectra related to Ti^{3+} disappeared. The center position of the Ti^{4+} emission and excitation spectra is the same as that in Figs. 6 and 7. These excitation spectra were fitted by two single Gaussians as performed in Figs. 6 and 7. Figure 13 also shows a continuous change of the emission spectra from 460 (for λ_{ex}=240 nm) to 520 nm (for λ_{ex}=310 nm) as a result of the superposition of the F^+ color center with Ti^{4+} via charge energy transfer. The ESR spectra determined before and after the annealing procedure on this sample are presented in Fig. 14, showing the absence of the resonance line related to Ti^{3+} ions in the thermally treated sample. This result confirms the assignments of the luminescence and excitation bands of Ti^{3+} ions and Ti^{4+} clusters.

E. The relationship among Ti^{3+}, Ti^{4+}, and Ti^{3+}-Ti^{4+} pairs

The existence of pairs involving Ti^{3+} and Ti^{4+} was verified by fitting the optical-absorption coefficient data shown in Fig. 1, which was performed by using the best fit parameters of the excitation bands and fixing the width and peak positions in the curves in Figs. 2 and 5–7. This procedure permits one to estimate the relative intensities of these bands,

TABLE II. Emission and excitation bands observed for undoped and TiO_2-doped LSCAS samples.

Sample	Excitation center (nm)	Emission center (nm)	Emission assignments
Undoped LSCAS	240	431	F kind color center
	325	527	F^+ color center
TiO_2-doped LSCAS	240	431	F kind color center
	271	486	$(TiO_6)^{8-}$
	338	640	Ti^{3+}
	540	Not observed	Ti^{4+}-Ti^{3+} pairs

which was impossible using the excitation experiment data. An additional band related to Ti^{3+}-Ti^{4+} pairs was also taken into account. Since it was not possible to perform deconvolution of this band by excitation and the contour plot procedure, we let its parameters free in the fitting procedure. Table II shows the obtained bands and the corresponding emission centers. Figure 15 shows an example to obtain the best fit for the absorption spectrum of the 3.5 wt % TiO_2-doped LSCAS. The areas of the Gaussians relative to Ti^{4+}, Ti^{3+}, and Ti^{3+}-Ti^{4+} pairs were obtained. This procedure was performed for all absorption curves of Fig. 1. Then, the results of the absorption areas versus the wavelength of the band centers were calculated as shown in Fig. 16. The areas of Ti^{3+} and Ti^{3+}-Ti^{4+} absorption bands as a function of [TiO_2] concentration presented a nonlinear behavior, while the Ti^{4+} band seems to increase almost linearly with the [TiO_2] concentration. This agrees with that is predicted by Eqs. (2) and (3) and Fig. 12.

In order to analyze the [Ti^{4+}] pairs that should be proportional to [Ti^{3+}][Ti^{4+}], we adopted a similar procedure such as that applied by Bausá *et al.*[34] to study titanium-doped phosphate glasses. The [Ti^{4+}] fraction in the sample is estimated taking into account the [Ti^{3+}] described by Eq. (2), resulting in

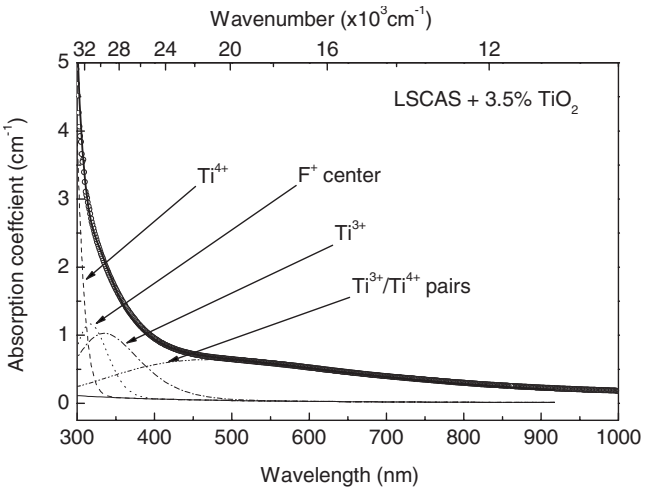

FIG. 15. Deconvolution of the optical-absorption spectrum of the 3.5 wt % TiO_2 LSCAS using those parameters obtained in the fitting of the excitation spectra.

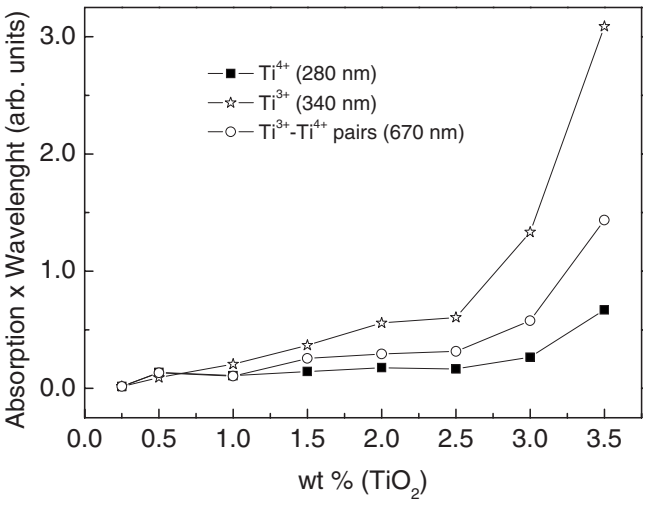

FIG. 16. Areas from the Gaussian fittings associated to Ti^{4+}, Ti^{3+}, and Ti^{3+}-Ti^{4+} pairs as a function of TiO_2 concentration.

$$[Ti^{4+}] = (1\text{-}C)[TiO_2]. \tag{5}$$

Therefore the $[Ti^{3+}][Ti^{4+}]$ can be written as

$$[Ti^{3+}][Ti^{4+}] = C(1\text{-}C)[TiO_2]^2. \tag{6}$$

Thus, the contribution of Ti^{3+}-Ti^{4+} pairs to the absorption spectra is nonlinear due to both the quadratic dependence with $[TiO_2]$ and the dependence with C as described in Eq. (3).

F. Proposed model to explain the long lifetime of Ti^{3+} ions

In our previous paper (Ref. 1), we proposed a model to explain the long lifetime observed for the Ti^{3+}-doped sample orange emission. The hypothesis was that the UV laser at 3.5 eV excites one electron of the Ti^{3+} ion ground state ($^2T_2$) to an excited band (^2E) from which it is trapped by a vacancy close to the conduction band (CB). Two possible mechanisms were proposed to describe the detrapping process via excitation of the Ti^{3+} (^2E) metastable band. The first was that the thermal energy at room temperature would promote the electron to the conduction band from where it relaxes back to a $(Ti^{3+})^+$ forming Ti^{3+} excited $[Ti^{3+}]^+$, which relaxes emitting one photon at 650 nm (1.9 eV). The second proposed route was the electron tunneling directly to the ^2E band from where the emission would occur. In order to try to better understand the detrapping process, in this work we performed an additional experiment using the photoconductivity technique.[31] No evidence of photoconductivity was observed in the sample when the excitation was performed at 355 nm. This fact suggests that instead of passing by the conduction band, the electron probably passes directly from the ^2E excited level to a shallow trap as illustrated in Fig. 17. After that it can be promoted back to $(Ti^{3+})^+$ forming Ti^{3+} excited ($[Ti^{3+}]*$), which relaxes from the ^2E to the $^2T_2$ level. Once this vacancy defect is located near the Ti^{3+} ion, a second possibility could be that the electron tunnels directly to the $(Ti^{3+})^+$ ^2E band from where the emission would occur. The following channels summarize these suggested processes:

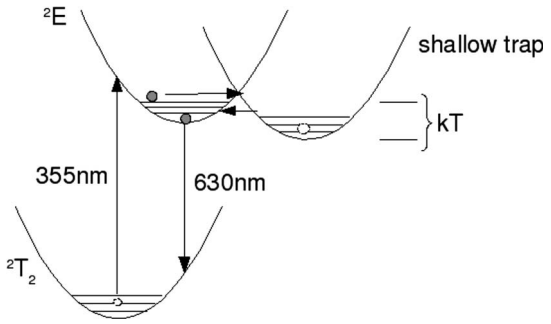

FIG. 17. Diagram of the energy bands taking into account the interaction between electron trap and Ti^{3+} ion in the LSCAS glass.

$$\text{first} \quad Ti^{3+}h\nu(350\ \text{nm}) \rightarrow (Ti^{3+})^+ + \{\text{electron in a hole center}\},$$

$$\text{second} \quad \begin{cases} \{\text{electron in a hole center}\} + kT + (Ti^{3+})^+ \rightarrow [Ti^{3+}]^* \\ \text{or} \\ \{\text{electron in a hole center}\} + \text{tunneling} + (Ti^{3+})^+ \rightarrow [Ti^{3+}]^*, \end{cases}$$

$$\text{third} \quad [Ti^{3+}]^* \rightarrow Ti^{3+}h\nu(\sim 650\ \text{nm}).$$

Thus it is clear that for higher temperatures the detrapped process is easily obtained due to kT, explaining the observed significant reduction in the lifetime ($\sim 90\ \mu s$) as can be observed in Fig. 10. At lower temperatures, the electrons remain trapped for a long period of time, which increases the luminescence decay time of the ^2E band. Therefore, the long lifetime of the luminescence may be due to the long period of trapping and not necessarily to the Ti^{3+} lifetime. This proposed mechanism is supported by the strong dependence of the lifetime with the temperature. This observation is consistent with the fact that the ^2E band for Ti^{3+}-doped materials has an expected lifetime on the order of microseconds, similar to the lifetime for the high-temperature region where the trap effect is minimized. The

schematic of the energy bands of this process is summarized in Fig. 17.

IV. CONCLUSIONS

In conclusion, in this work we performed a comprehensive investigation of the spectroscopic properties of OH^- free Ti-doped LSCAS glass. Color centers were formed in the glass during the UV excitation presenting emissions at 431 and 527 nm for excitations at 240 and 320 nm, respectively. The spectroscopic results showed that the increase in the TiO_2 amount in the sample favored the formation of Ti^{3+} ions. After annealing of the doped samples at 850 °C for 24 h, the 640 nm emission band and the ESR signal from Ti^{3+} ions disappeared, confirming the assignment of the emission bands to the charge-transfer processes between Ti^{3+} and Ti^{4+}. The results suggest that the oxygen ions are responsible for the reduction in Ti^{3+} and the consequent increase in the Ti^{4+} amount in the glass, indicating that these ions enter into the lattice changing the valence of the Ti and breaking bonds inside the glass. An additional and important finding refers to the long lifetime of Ti^{3+} ions in this glass (~2.0 ms at 77 K and 170 μs at room temperature), which was associated to a possible interaction between defects and Ti^{3+} ions. This mechanism is supported by the observed color center formation in the glass. The absence of photoconductivity and the presence of blue emission under 355 nm excitation is an indication that this glass presents insignificant excited-state absorption. Further studies are warranted to evaluate the possibility of using this material for laser application.

ACKNOWLEDGMENTS

The authors are thankful to CNPq, Fundação Araucária, CAPES/COFECUB (Brazil/France cooperation) under Grant No. 565/07, and CNRS-UCBLyon1 for the financial support of this work.

*luishca@uems.br

[1] L. H. C. Andrade, S. M. Lima, A. Novatski, P. T. Udo, N. G. C. Astrath, A. N. Medina, A. C. Bento, M. L. Baesso, Y. Guyot, and G. Boulon, Phys. Rev. Lett. **100**, 027402 (2008).
[2] S. M. Jacobsen and H. U. Güdel, J. Lumin. **43**, 125 (1989).
[3] T. C. Brunold, H. U. Güdel, and A. A. Kaminskii, Chem. Phys. Lett. **271**, 327 (1997).
[4] M. F. Hazenkamp and H. U. Güdel, Chem. Phys. Lett. **251**, 301 (1996).
[5] T. C. Brunold, M. F. Hazenkamp, and H. U. Güdel, J. Lumin. **72-74**, 164 (1997).
[6] D. Ehrentraut, M. Pollnau, and S. Kück, Appl. Phys. B: Lasers Opt. **75**, 59 (2002).
[7] T. C. Brunold and H. U. Güdel, Inorg. Chem. **36**, 1946 (1997).
[8] P. F. Moulton, J. Opt. Soc. Am. B **3**, 125 (1986).
[9] P. Alberts, E. Stark, and G. Huber, J. Opt. Soc. Am. B **3**, 134 (1986).
[10] L. D. Jung, F. X. Kärtner, N. Matuschek, D. H. Sutter, F. Morier-Genoud, G. Zhang, U. Keller, V. Scheuer, M. Tilsch, and T. Tschudi, Opt. Lett. **22**, 1009 (1997).
[11] W. Jia, Y. Wang, I. R. Figueroa, and H. Liu, Colloids Surf., A **179**, 185 (2001).
[12] T. C. Brunold and H. U. Güdel, Chem. Phys. Lett. **249**, 77 (1996).
[13] M. F. Hazenkamp and H. U. Güdel, J. Lumin. **69**, 235 (1996).
[14] T. Maksimova, K. Hermanowicz, L. Macalik, and J. Hanuza, J. Mol. Struct. **563**, 353 (2001).
[15] W. C. Wong, D. S. McClure, S. A. Basun, and M. R. Kokta, Phys. Rev. B **51**, 5682 (1995).
[16] W. C. Wong, D. S. McClure, S. A. Basun, and M. R. Kokta, Phys. Rev. B **51**, 5693 (1995).
[17] S. A. Basun, T. Danger, A. A. Kaplyanskii, D. S. McClure, K. Petermann, and W. C. Wong, Phys. Rev. B **54**, 6141 (1996).
[18] M. Yamaga, T. Yosida, S. Hara, N. Kodama, and B. Henderson, J. Appl. Phys. **75**, 1111 (1994).
[19] T. Wegner and K. Peterman, Appl. Phys. B: Photophys. Laser Chem. **B49**, 275 (1989).
[20] T. Sato, M. Shirai, K. Tanakab, Y. Kawabe, and E. Hanamura, J. Lumin. **114**, 155 (2005).
[21] T. Danger, K. Petermann, N. Schwentner, G. Sliwinski, and W. C. Wong, J. Lumin. **72-74**, 171 (1997).
[22] J. A. Duffy and M. D. Ingram, J. Am. Chem. Soc. **93**, 6448 (1971).
[23] S. Tanabe, T. Ohyagi, T. Hanada, and N. Soga, J. Ceram. Soc. Jpn. **101**, 74 (1993).
[24] M. L. Baesso, A. C. Bento, A. R. Duarte, A. M. Neto, L. C. M. Miranda, J. A. Sampaio, T. Catunda, S. Gama, and F. C. Gandra, J. Appl. Phys. **85**, 8112 (1999).
[25] M. L. Baesso, A. C. Bento, A. A. Andrade, J. A. Sampaio, E. Pecoraro, L. A. O. Nunes, T. Catunda, and S. Gama, Phys. Rev. B **57**, 10545 (1998).
[26] J. E. Shelby, J. Am. Ceram. Soc. **68**, 155 (1985).
[27] J. A. Sampaio, T. Catunda, F. G. C. Gandra, S. Gama, A. C. Bento, L. C. M. Miranda, and M. L. Baesso, J. Non-Cryst. Solids **247**, 196 (1999).
[28] J. A. Sampaio, T. Catunda, A. A. Coelho, S. Gama, A. C. Bento, L. C. M. Miranda, and M. L. Baesso, J. Non-Cryst. Solids **273**, 239 (2000).
[29] S. L. Oliveira, S. M. Lima, T. Catunda, H. Vargas, L. A. O. Nunes, J. H. Rohling, A. C. Bento, and M. L. Baesso, J. Phys. IV **125**, 193 (2005).
[30] R. Reisfeld, A. Kisilev, A. Buch, and M. Ish-Shalom, J. Non-Cryst. Solids **91**, 333 (1987).
[31] M.-F. Joubert, S. A. Kazanskii, Y. Guyot, J.-C. Gâcon, and C. Pédrini, Phys. Rev. B **69**, 165217 (2004).
[32] N. Abd El-Shafi and M. M. Morsi, J. Mater. Sci. **32**, 5185 (1997).
[33] P. Yang, M. Lü, D. Xu, D. Yuan, C. Song, and G. Zhou, Appl. Phys. A: Mater. Sci. Process. **74**, 525 (2002).
[34] L. E. Bausá, J. Garcia Sole, A. Duran, and J. M. Fernández Navarro, J. Non-Cryst. Solids **127**, 267 (1991).
[35] Z. P. Argüello, S. A. Bilac, J. I. Cisneros, M. Tomyaiama, P.

Donoso, and L. C. M. Miranda, Glass Technol. **22**, 186 (1981).
[36] H. Hosono, N. Asada, and Y. Abe, J. Appl. Phys. **67**, 2840 (1990).
[37] M. Yamaga, B. Henderson, T. Yosida, N. Kodama, and Y. Inoue, Phys. Rev. B **51**, 3438 (1995).
[38] M. J. Norman, L. D. Morpeth, and J. C. McCallum, Mater. Sci. Eng., B **106**, 257 (2004).
[39] M. Grinberg, A. Mandelis, K. Fjeldsted, and A. Othonos, Phys. Rev. B **48**, 5922 (1993).
[40] M. Herren, H. Nishiuchi, and M. Morita, J. Chem. Phys. **101**, 4461 (1994).
[41] V. I. Baryshnikov, J. Kvapil, N. Sarukura, and Y. Segawa, J. Lumin. **72-74**, 157 (1997).
[42] M. Akiyama, C. Xu, and K. Nonaka, Appl. Phys. Lett. **81**, 457 (2002).
[43] M. Akiyama, C. Xu, K. Nonaka, and T. Watanabe, Appl. Phys. Lett. **73**, 3046 (1998).
[44] M. Akiyama, C. Xu, H. Matsui, and K. Nonaka, Appl. Phys. Lett. **75**, 2548 (1999).
[45] M. Yamaga, T. Yosida, Y. Naitoh, and N. Kodama, J. Phys.: Condens. Matter **6**, 4381 (1994).
[46] G. Wang, H. G. Gallagher, T. P. J. Han, B. Henderson, M. Yamaga, and T. Yosida, J. Phys.: Condens. Matter **9**, 1649 (1997).
[47] J. Dziesiaty, M. U. Lehr, P. Peka, A. Klimakow, S. Müuller, and H.-J. Schulz, Eur. Phys. J. B **4**, 269 (1998).
[48] Kenji Morinaga, Hideki Yoshida, and Hiromichi Takebe, J. Am. Ceram. Soc. **77**, 3113 (1994).